

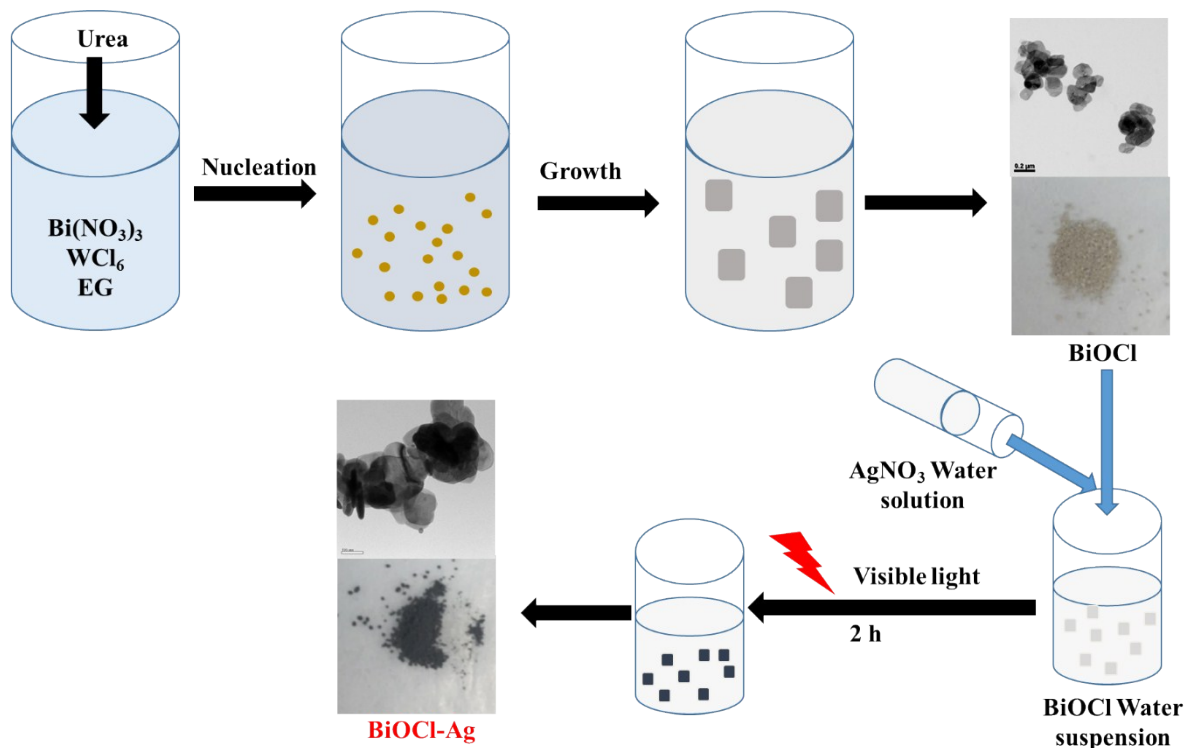
**Deposition of Silver nanoparticles onto two dimensional BiOCl nanodisc for enhanced
visible light photocatalytic and biocidal activities**

Wenyu Zhu^{ab}, Zhong Li^c, Yan Zhou^{ab}, Xiaoli Yan^{ad*}*

- a. School of Civil and Environmental Engineering, Nanyang Technological University, 50 Nanyang Avenue, Singapore 639798, Republic of Singapore
- b. Nanyang Environment and Water Research Institute (NEWRI), Nanyang Technological University, 1 Cleantech Loop, CleanTech One, Singapore 637141, Republic of Singapore
- c. School of Mechanical and Aerospace Engineering, Nanyang Technological University, 50 Nanyang Avenue, Singapore 639798, Republic of Singapore
- d. Environmental and Water Technology Centre of Innovation, Ngee Ann Polytechnic, 535 Clementi Road, Singapore 599489, Republic of Singapore (Current address)

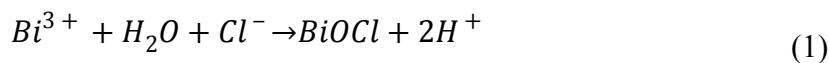
* Corresponding author(s):

Email: zhouyan@ntu.edu.sg (Yan Zhou); xlyan@ntu.edu.sg, yan_xiaoli@np.edu.sg (Xiaoli Yan)



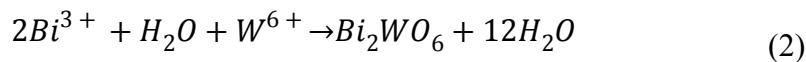
Scheme S1. Schematic diagram of the synthesis of BiOCl and BiOCl-Ag.

The possible growth mechanism of 2D BiOCl in EG solution has been proposed by other researchers and can be explained by Ostwald ripening where small BiOCl crystalline nuclei appeared in the EG solution at high temperature and auto-generated vapor pressure followed the chemical reaction in Eq. S1.¹⁻³ By Ostwald ripening, the small BiOCl nuclei aggregated together and grew into larger 2D BiOCl nanodisks as shown in Scheme S1.



However, in this process, many factors were found to be able to affect the generation of final products such as Bi(NO₃)₃·5H₂O to WCl₆ ratio, and addition of water. To verify the possible influence of Bi(NO₃)₃·5H₂O to WCl₆ ratio, 0.5 mmol WCl₆ and 1 mmol Bi(NO₃)₃·5H₂O were

used as precursors where BiOCl-Bi₂WO₆ microflowers were produced which is in correspondence with previous reports.⁴⁻⁶ In these studies, the appearance of Bi₂WO₆ was attributed to factors like amount of urea, pH, temperature, thermodynamical stability of BiOCl and Bi₂WO₆, as well as chemical and physical properties of solvents. While in our study, we found that the addition of water would affect the final products significantly. When the Bi(NO₃)₃·5H₂O to WCl₆ ratio was kept at 1:1 and different volume of water (1mL and 5 mL) was added, the final products were found to be pure Bi₂WO₆ as presented in Fig.S1. No peak belonging to BiOCl was observed and the XRD patterns well followed the orthorhombic structure of Bi₂WO₆ (JCPD file No. 39-0256). Therefore, water can be regarded as an important factor influencing the formation process of BiOCl and Bi₂WO₆. In particular, when no external water was added and Bi(NO₃)₃·5H₂O to WCl₆ ratio was 1:1, EG could react with WCl₆ to form [EG-W]⁶⁺ composites, which could effectively inhibit the hydrolysis of WCl₆ since the small amount of crystal water of Bi(NO₃)₃·5H₂O was not able to sufficiently hydrolyze WCl₆.^{7, 8} As a result, only BiOCl was produced following Eq. S(1). However, when external water was added, the hydrolysis of WCl₆ would be remarkably accelerated and OH⁻ would take place of Cl⁻ to form W-OH which became the dominant reaction and subsequently led to the generation of Bi₂WO₆ rather than BiOCl (Eq S(2)). When Bi(NO₃)₃·5H₂O to WCl₆ ratio was 2:1, the crystal water of Bi(NO₃)₃·5H₂O could partially hydrolyze WCl₆ and as a result, Bi₂WO₆ would appear in the final products. However, our understanding is still quite limited and further study is still need to reveal the growth mechanism of BiOCl, Bi₂WO₆ and their heterojunctions in EG.



Bi/W ratio	Water (mL)	Urea (mmol)	Chemical Compositions	Shape
1:1	—	6	BiOCl	Nanodiscs (Fig. S1 (a))
2:1	—	6	BiOCl-Bi ₂ WO ₆	Microflowers (Fig. S1 (b))
1:1	1-5	6	Bi ₂ WO ₆	Microflowers (Fig. S1 (c,d))

Table S1 The products prepared under different conditions at 120°C for 4h

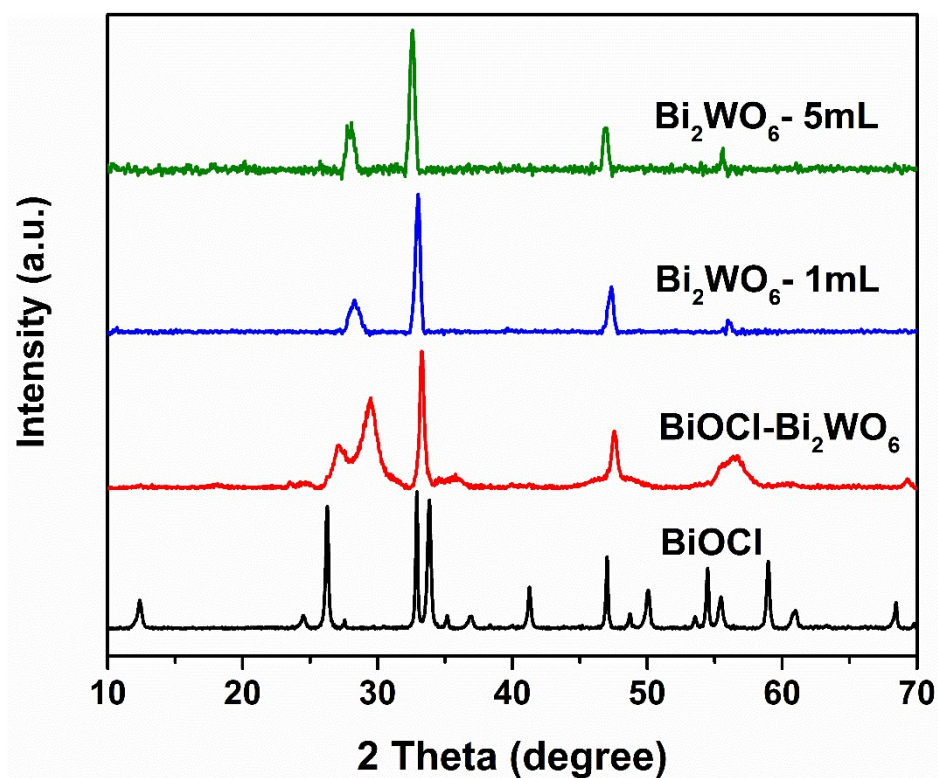


Fig. S1 XRD patterns of products synthesized under different conditions.

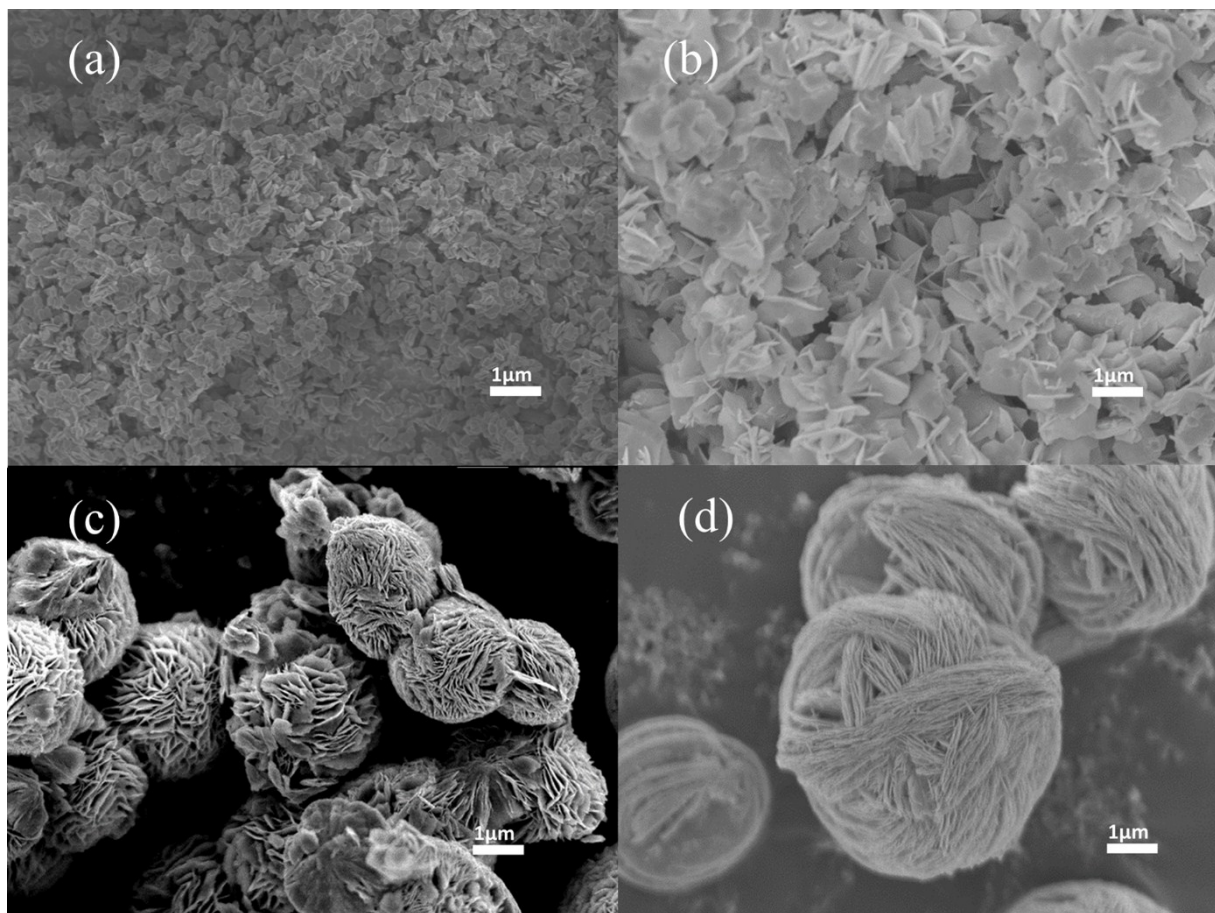


Fig. S2 SEM images of products synthesized under different conditions: BiOCl nanodiscs (a); BiOCl-Bi₂WO₆ microflowers (b) and Bi₂WO₆ nanoflowers with addition of 1 mL water (c) and 5 mL water (d).

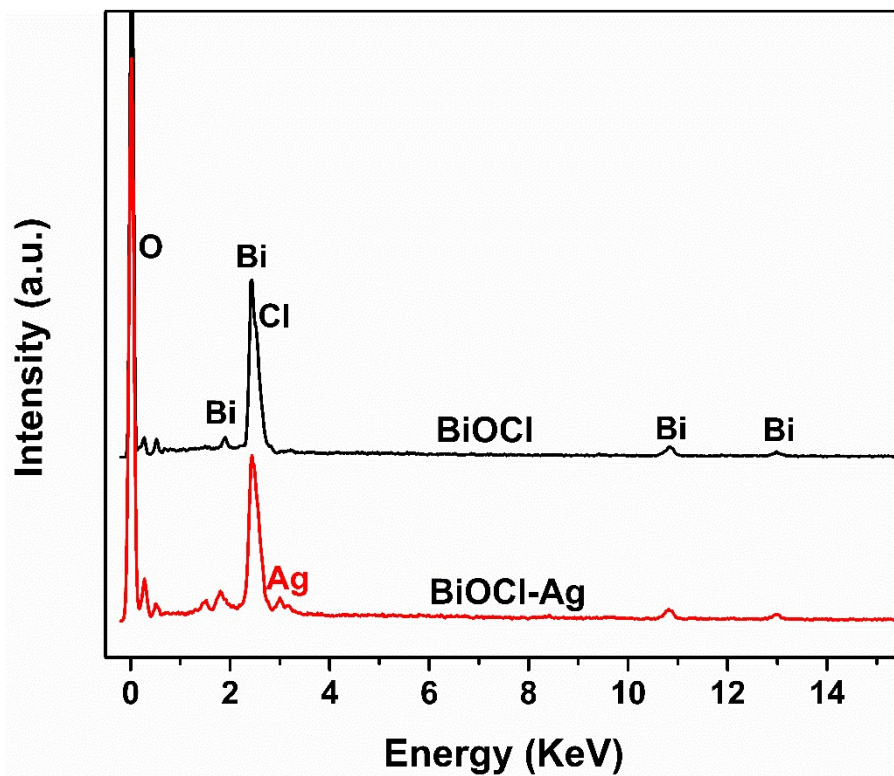


Fig. S3 EDX patterns of BiOCl and BiOCl-Ag.

In addition to XPS, EDX is also a useful method to study the element composition of nanomaterials. As displayed in Fig. S3, only Bi, O, and Cl were observed from BiOCl sample. By contrast, new peaks at round 3 KeV belong to Ag were found from BiOCl-Ag, indicating Ag deposition on BiOCl.

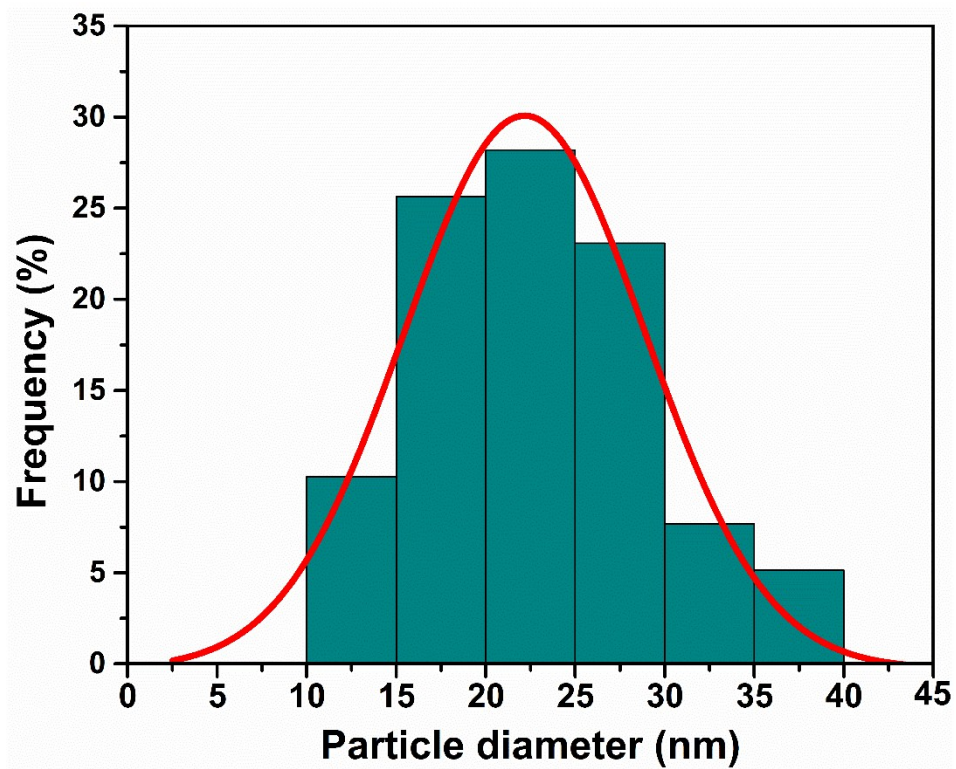


Fig. S4 Ag NPs (nanoparticles) size distribution on BiOCl nanodiscs.

After 2 h irradiation, the size of Ag NPs on the BiOCl nanodiscs was mainly in the range of 15 to 35 nm.

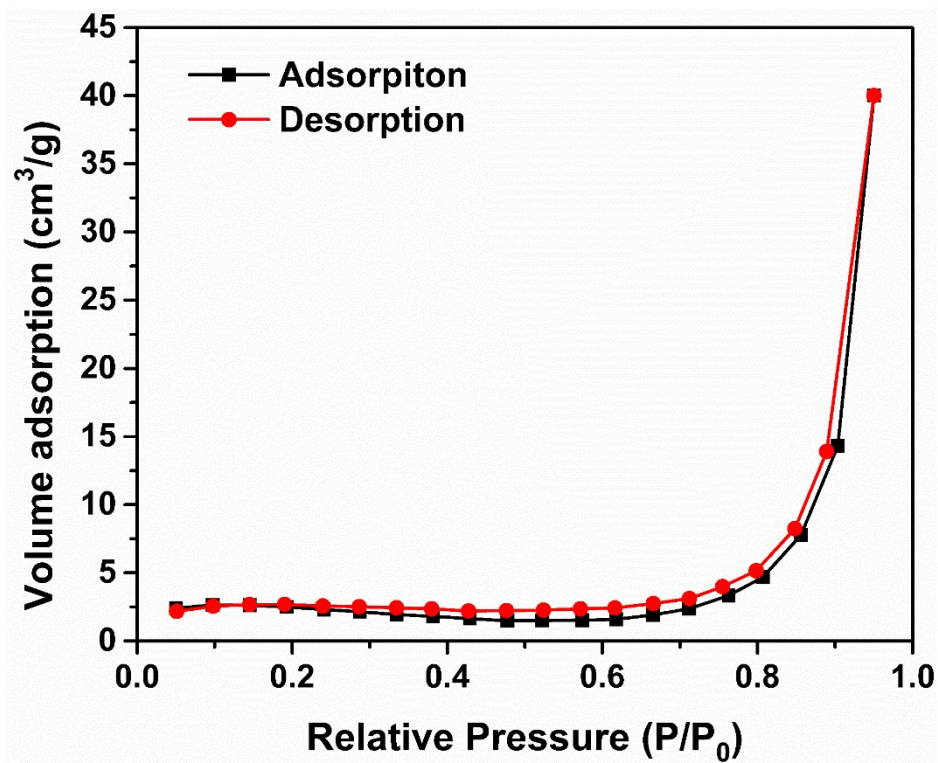


Fig. S5 N₂ adsorption-desorption isotherms of BiOCl nanodiscs.

The specific surface area of BiOCl nanodiscs was measured with nitrogen adsorption and desorption isotherms as illustrated in Fig. S5. The isotherms can be nearly categorized as type III and the BET surface area of BiOCl calculated from the result of N₂ isotherms was 6.54 m² g⁻¹.

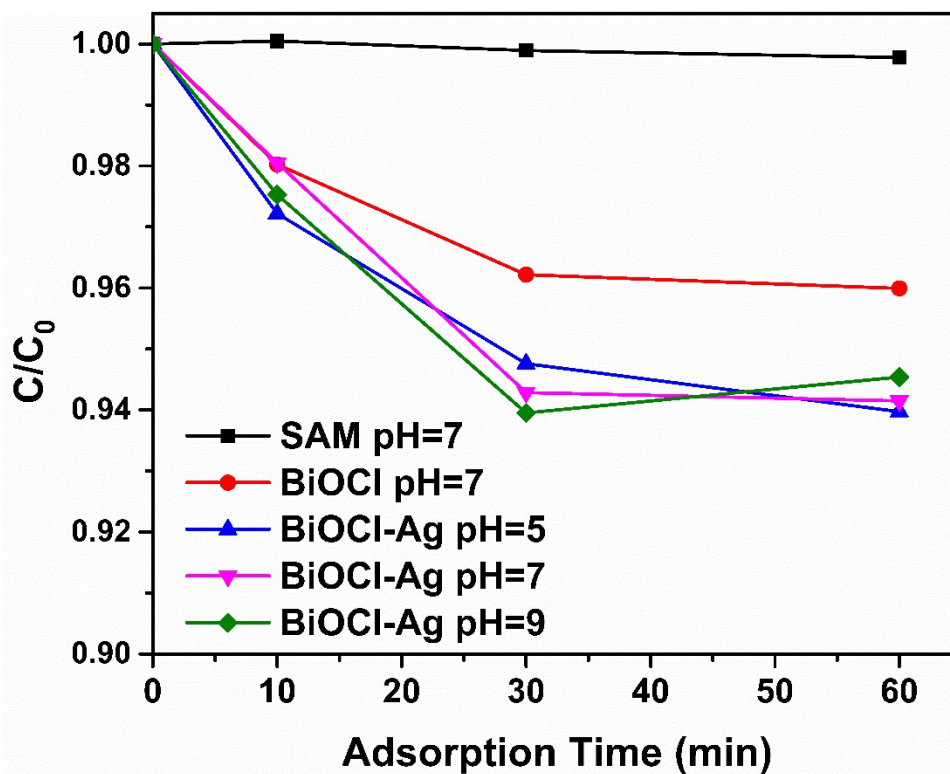


Fig. S6 Adsorption of SAM in 1 h under dark, SAM=10 mg L⁻¹ and catalyst dosage=1.0 g L⁻¹.

The adsorption equilibriums of SAM of BiOCl and BiOCl-Ag were tested within 1 h, and results show only around 5% of SAM were adsorbed on the catalysts and the equilibrium could be successfully achieved in 60 min. This relatively low adsorption ability also confirms that the decline of SAM concentration during the light irradiation was the result of photo-degradation rather than simply adsorption on the catalysts.

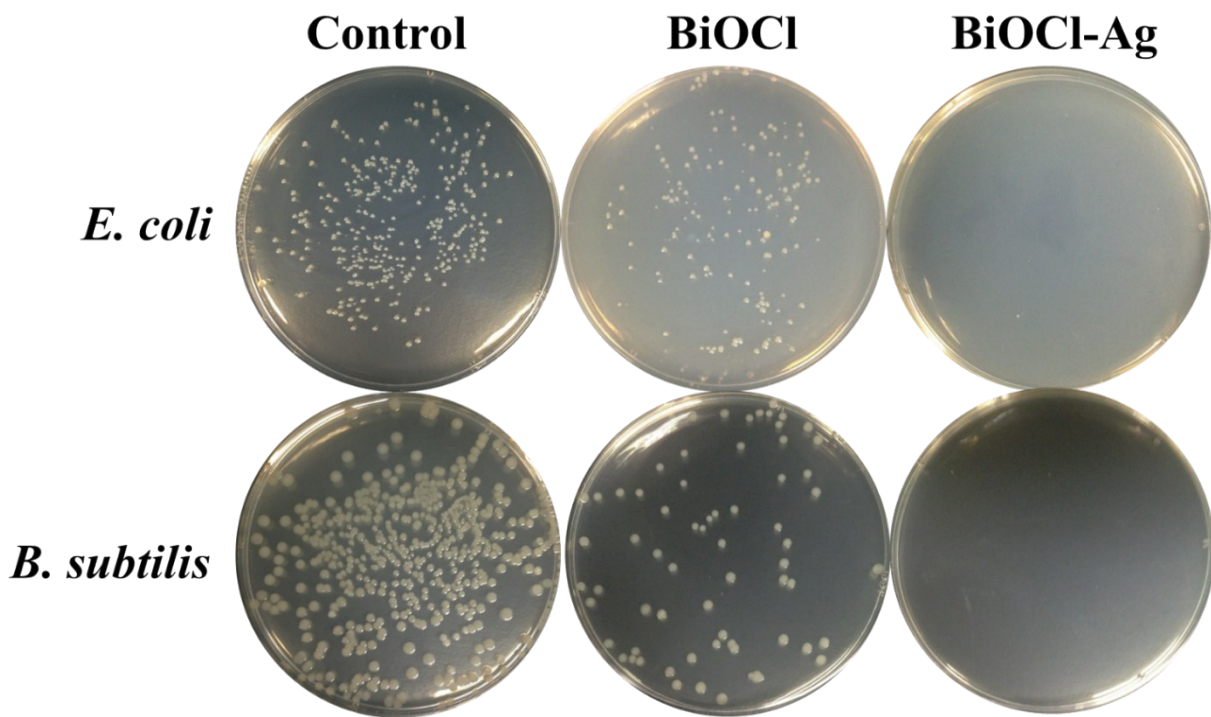


Fig. S7 Photographs of colony formation of *E. coli* and *B. subtilis* treated by 1.0 g L^{-1} BiOCl and BiOCl-Ag for 2h under visible light irradiation. Bacterial colonies formed without adding any catalyst was used as control.

The bacterial colonies formed on the LB agar mediums were observed as presented in Fig. S7. For both *E. coli* and *B. subtilis*, no colony was spotted after the cells were treated by BiOCl-Ag for 2 h, suggesting that BiOCl-Ag has a strong and efficient inactivation performance under visible light irradiation. By contrast, a number of colonies were found on LB agar mediums incubated by cells treated with BiOCl. Such huge difference can be explained by the different antibacterial mechanisms. The main contributor to antibacterial activity of BiOCl under visible light are reactive oxygen species (ROS) generated during the photocatalytic process. In the case of BiOCl-Ag, the enhanced photocatalytic activity could create more ROS, leading to the

improved antibacterial performance. Moreover, the excellent antibacterial effect of Ag would also contribute to the biocidal performance of BiOCl-Ag.

Initial pH (± 0.2)	Ag leaching (mg L^{-1})
5	0.08
7	0.06
9	0.06

Table S2 Ag leaching after 5 h visible light irradiation at different initial pH.

According to the regulation established by USA Environmental Protection Agency (EPA), the secondary maximum contaminant level (SMCL) of Ag is 0.1 mg L^{-1} ⁹. The concentrations of Ag leaching from different testing conditions were summarized in Table S2, and it is clear that all of them were below the SMCL. This suggests that the usage of BiOCl-Ag as photocatalyst would not cause negative influence on water quality.

Reference

1. L.-P. Zhu, G.-H. Liao, N.-C. Bing, L.-L. Wang, Y. Yang and H.-Y. Xie, *CrystEngComm*, 2010, **12**, 3791.
2. X. Xiao, R. Hao, M. Liang, X. Zuo, J. Nan, L. Li and W. Zhang, *Journal of hazardous materials*, 2012, **233-234**, 122-130.
3. P. Ye, J. Xie, Y. He, L. Zhang, T. Wu and Y. Wu, *Materials Letters*, 2013, **108**, 168-171.
4. J. Cheng, S. Shi, T. Tang, S. Tian, W. Yang and D. Zeng, *Journal of Alloys and Compounds*, 2015, **643**, 159-166.
5. W. Yang, B. Ma, W. Wang, Y. Wen, D. Zeng and B. Shan, *Physical chemistry chemical physics : PCCP*, 2013, **15**, 19387-19394.
6. Z. Cui, J. Zhou, D. Zeng, J. Zhang, W. Fa and Z. Zheng, *Materials Technology: Advanced Performance Materials*, 2015, **30**, 23-27.
7. J. Liu, S. Yu, W. Zhu and X. Yan, *Applied Catalysis A: General*, 2015, DOI: 10.1016/j.apcata.2015.04.033.
8. Z. Wang, M. Hu, Y. Wei, J. Liu and Y. Qin, *Applied Surface Science*, 2016, **362**, 525-531.
9. S. S. Tan, Y. N. Teo and E. T. Kool, *Organic letters*, 2010, **12**, 4820-4823.